Stochastic opinion formation in scale-free networks

M. Bartolozzi,[1] D. B. Leinweber,[1] and A. W. Thomas[1,2]
[1]*Special Research Centre for the Subatomic Structure of Matter (CSSM), University of Adelaide, Adelaide, South Australia 5005, Australia*
[2]*Jefferson Laboratory, 12000 Jefferson Avenue, Newport News, Virginia 23606, USA*
(Received 26 April 2005; revised manuscript received 17 August 2005; published 13 October 2005)

The dynamics of opinion formation in large groups of people is a complex nonlinear phenomenon whose investigation is just beginning. Both collective behavior and personal views play an important role in this mechanism. In the present work we mimic the dynamics of opinion formation of a group of agents, represented by two states ±1, as a stochastic response of each agent to the opinion of his/her neighbors in the social network and to feedback from the average opinion of the whole. In the light of recent studies, a scale-free Barabási-Albert network has been selected to simulate the topology of the interactions. A turbulentlike dynamics, characterized by an intermittent behavior, is observed for a certain range of the model parameters. The problem of uncertainty in decision taking is also addressed both from a topological point of view, using random and targeted removal of agents from the network, and by implementing a three-state model, where the third state, zero, is related to the information available to each agent. Finally, the results of the model are tested against the best known network of social interactions: the stock market. A time series of daily closures of the Dow-Jones index has been used as an indicator of the possible applicability of our model in the financial context. Good qualitative agreement is found.

DOI: 10.1103/PhysRevE.72.046113 PACS number(s): 02.50.−r, 02.60.Cb, 05.45.−a, 05.45.Tp

I. INTRODUCTION

Systems composed of many parts that interact with each other in a nontrivial way are often referred to as *complex systems*. The social relations between individuals can perhaps be included in this category. An intriguing issue concerns the role played by the topological structure of the social network in governing the dynamical behavior of the system.

Recent studies of the topological properties of interactions in different biological, social, and technological systems have made it possible to shed some light on the basic principles of structural self-organization. A few examples include food webs [1], power grids and neural networks [2,3], cellular networks [4], sexual contacts [5], Internet routers [6], the World Wide Web [7], actor collaborations [2,3,8,9], the citation networks of scientists [10], and the stock market [11]. Although different in the underlying interaction dynamics or *microphysics*, all these networks have shown a tendency to self-organize in structures that share common features. In particular, the number of connections k for each element, or node, of the network follow a power law distribution $P(k) \sim k^{-\alpha}$. Networks that satisfy this property are referred to as *scale-free* (SF) networks. In addition many of these networks are characterized by a high clustering coefficient C, in comparison with random graphs [12]. The clustering coefficient C is computed as the average of local clustering C_i for the ith node, defined as

$$C_i = \frac{2y_i}{z_i(z_i - 1)}, \tag{1}$$

where z_i is the total number of nodes linked to the site i and y_i is the total number of links between those nodes. As a consequence both C_i and C lie in the interval [0,1]. The high level of clustering found supports the idea that a *herding* phenomenon is a common feature in social and biological communities.

Numerical studies on SF networks have demonstrated how the topology plays a fundamental role in infection spreading [13] and tolerance against random and preferential node removal [14]. A detailed description of the progress in this emerging field of statistical mechanics can be found in the recent reviews of Refs. [15,16]. In the present work we investigate the implication of a scale-free topology in a stochastic opinion formation model. Similar versions of this model have been tested in regular lattices [17,18] and percolation clusters [19]. These models adopt a mean field approach where the interactions are extended between all the individuals in the lattice or cluster, respectively. In contrast, our simulation focuses on the role of short-range first-neighbor interactions for cases where the topological structure of the interactions is not trivial.

In the next section we describe the model used for the simulation. In Sec. III we show the results obtained numerically while in Sec. IV we investigate the importance of failures in the network during the process of opinion formation. In Sec. V the two-state model is extended to three states and the numerical results are compared. In Secs. VI and VII we test the results of our simulations against the best known social network: the stock market. In particular the time series of average opinion fluctuations obtained with the model is compared with the time series of price variations for the Dow-Jones index from 13/1/1930 to 13/4/2004. The final section presents further discussion and conclusions.

II. THE MODEL

In the present work we investigate the opinion formation process of a group of N individuals, represented by nodes on

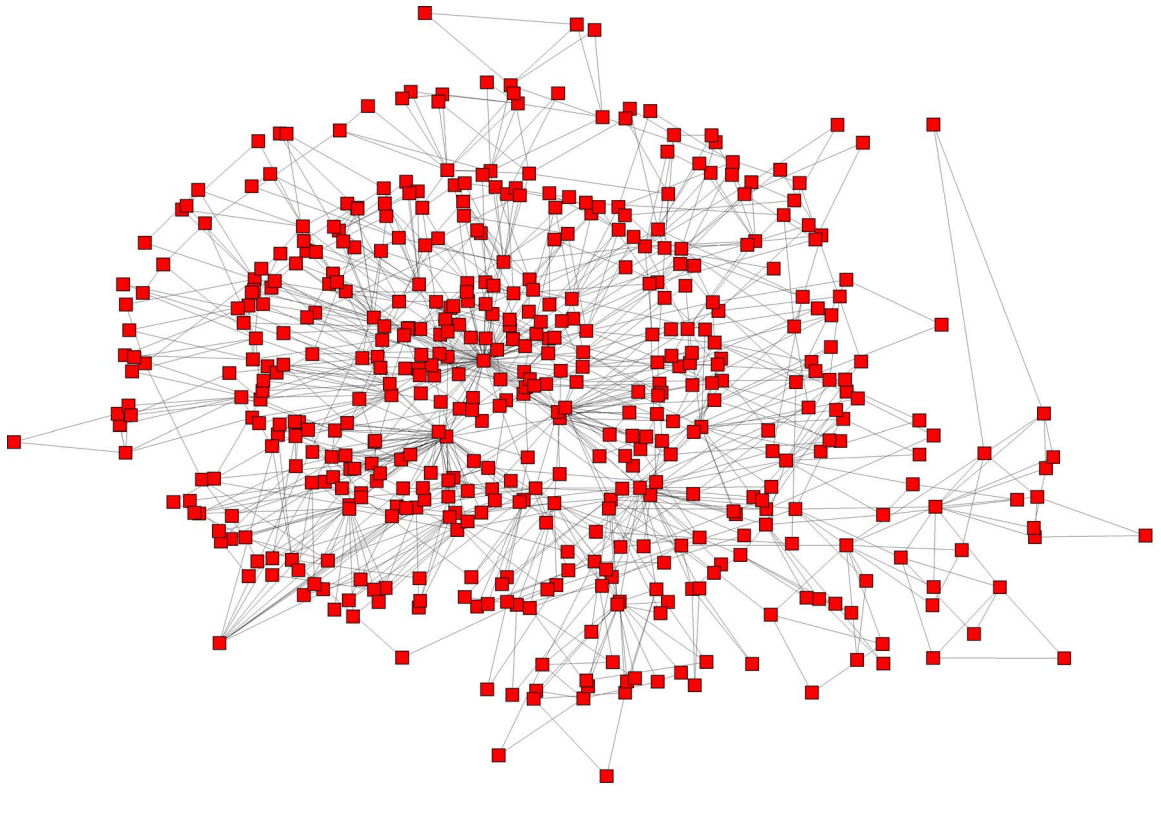

FIG. 1. (Color online). Example of a scale-free network. The number of nodes is 500 with clustering probability $\theta=0.9$ and $m_0=m=2$, so that each new node is linked twice. The number of nodes has been kept small in order to preserve the clarity of the plot. Note that, for such small networks, a large scale invariant range is obtained only if one considers the ensemble average over several realizations. This plot has been realized with the PAJEK software [21].

a SF network. The mechanism of opinion formation is simulated using stochastic heat bath dynamics with feedback. The opinion of each agent is of a Boolean type. That is, at each discrete time step t, the opinion is represented by one of two possible states (or spin orientations), namely, $\sigma_i(t)=\pm 1$, for the ith agent. A practical example could be the decision to buy, $\sigma_i(t)=+1$, or sell, $\sigma_i(t)=-1$, a stock in a virtual stock market.

In order to mimic the scale-free network topology we make use of the Barabási-Albert model [9]. This is based on two main assumption: (i) linear growth and (ii) preferential attachment. In practice the network is initialized with m_0 disconnected nodes. At each step a new node with m edges is added to the preexisting network. The probability that an edge of the new node is linked with the ith node is expressed by $\Pi(k_i)=k_i/\Sigma_j k_j$. The iteration of this preferential growing process yields a scale-free network $P(k)\sim k^{-\alpha}$ where $\alpha=3$.

It is worth noting that the Barabási-Albert model cannot reproduce a high clustering coefficient. In fact, the value of this coefficient depends on the total number of nodes in the network [15] and in the thermodynamic limit, $N\to\infty$, $C\to 0$. In principle the observed local clustering can play an important role in the opinion formation of groups of people, independent of their total number. In order to account for this, we introduce a further step in the growth process, namely, the triad formation proposed by Holme and Kim [20]. In this case, if the new added node is linked with an older node i having other links, then with a certain probability θ the next link of the new node, if any remain, will be added to a randomly selected neighbor of node i. This method of introducing friends to friends, while preserving the scale-free nature of the networks, generates high clustering coefficients that do not depend on the number of nodes in the network. The only tunable parameter that changes the value of the clustering coefficient is the clustering probability θ. An example of a SF network generated with this algorithm is shown in Fig. 1 for 500 nodes.[1]

Once the scale-free network has been built, we randomly assign the spin values ± 1 to every node and start the simulation of opinion formation. We neglect, in the first approximation, the network dynamics. This is equivalent to assuming that the time scale for evolving the network is much longer that the time needed for people to make a decision.

The dynamics of the spins follows a stochastic process that mimics the human uncertainty in decision making [18,19]. Values are updated synchronously according to a local probabilistic rule: $\sigma_i(t+1)=+1$ with probability p_i and $\sigma_i(t+1)=-1$ with probability $1-p_i$. The probability p_i is determined, by analogy with heat bath dynamics with formal temperature $k_BT=1$, by

[1]Another model for acquaintance networks, showing properties similar to the one presented in this work, has been proposed by Davidsen *et al.* [22].

$$p_i(t) = \frac{1}{1 + e^{-2I_i(t)}}, \tag{2}$$

where the local field $I_i(t)$ is

$$I_i(t) = a\xi(t)\tilde{N}_i^{-1}\sum_{j=1}^{\tilde{N}_i}\sigma_j(t) + h_i\eta_i(t)r(t). \tag{3}$$

The first term on the right-hand side of Eq. (3) represents the time dependent interaction strengths between the node i and his/her $\tilde{N}_i$ information sources, which are the first neighbors in the network. The second term instead reflects the personal reaction to the system feedback, that is, the average opinion,

$$r(t) = \frac{1}{N}\sum_{j=1}^{N}\sigma_j(t), \tag{4}$$

resulting from the previous time step. The terms $\xi(t)$ and $\eta_i(t)$ are random variables uniformly distributed in the interval $(-1,1)$ with no correlation in time nor in the network. They represent the conviction, at time t, with which agent i responds to his/her group (common for all the agents) and the global opinion of the network, respectively. The strength term a is constant and common for the whole network, while h_i is specifically chosen for every individual from a uniform distribution in $(0,\kappa)$ and are both constant in the dynamics of the system. By varying the parameter κ we can give more or less weight to the role of feedback in the model. The strength coefficients a and h_i in the local field I_i, characterizing the attributes of the agents, play a key role in the dynamics of the model. They represent the relative importance that each agent of the network gives, respectively, to his/her group and to the variation of the average opinion itself.

III. NUMERICAL SIMULATIONS

At first we investigate the importance of the group strength a by fixing $\kappa=a$. In this case the dynamical behavior is similar to that found in the stock market context in Refs. [17–19]. For $a \lesssim 1$ the resulting time series of average opinion is largely uncorrelated Gaussian noise with no particularly interesting features, as illustrated in Fig. 2(a).

As soon as we exceed the value of $a \approx 1$ a turbulentlike regime sets in, characterized by large intermittent fluctuations, as illustrated in Figs. 2(b) → Fig. 2(d). These large fluctuations, or *coherent events*, can be interpreted in terms of a multiplicative stochastic process with a weak additive noise background [18,23]. For $a > 2.7$ we observe that the bursts of the time series begin to saturate the bounds $-1 \leqslant r \leqslant 1$.

In Fig. 3 we plot the probability distribution functions (PDFs) associated with the time series of Fig. 2. The large fluctuations, for a greater than ≈ 1, are reflected in the fat tails of the relative PDFs. Decreasing the value of a, and so the number of coherent events, the PDF converges to a Gaussian distribution generated by a random Poisson process.

The personal response to the change in the average opinion also plays an important role in the turbulentlike regime

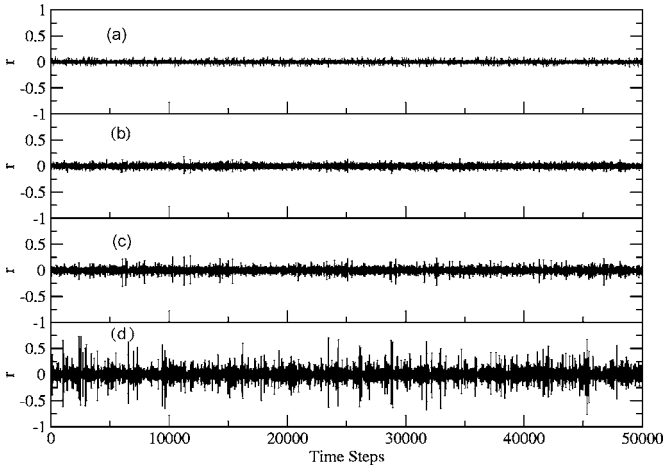

FIG. 2. Time series of the average opinion r for different values of the group interaction strength parameter a: a= (i) 0.8, (ii) 1.5, (iii) 1.8, and (iv) 2.3. The parameters used for the simulations are $N=10^4$ nodes, clustering probability $\theta=0.9$, initial nodes and links per new node $m_0=m=5$, and we take the upper bound of the distribution of personal response strengths equal to the group interaction strength, that is, $\kappa=a$. The results involve ten realizations of the scale-free network each displayed for 5000 time steps. For values of a greater than 1 a turbulentlike state, characterized by large fluctuations, starts to appear in the process of opinion formation. The clustering probability $\theta=0.9$, related to the triad formation in the network, fixes the clustering coefficient to $C \approx 0.39$. This value is similar to that found for many real systems [15,16].

of the simulation. In order to study the impact of this term on the dynamics we change the parameter κ while keeping a fixed at 1.8. The results are summarized by the PDF plots in Fig. 4. For $\kappa=0$ the behavior of the time series is still turbulentlike, underlying how the network group interaction is, in

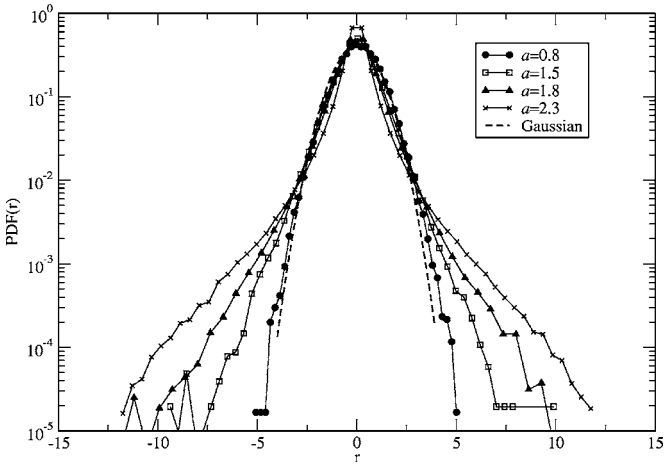

FIG. 3. PDFs of the time series relative to Fig. 2. The shapes of the distributions converge to a Gaussian for small values of the group interaction strength $a=\kappa$. A Gaussian distribution is also plotted for comparison. All the PDFs in this paper are obtained over 50 realizations of the SF network. In order to compare the fluctuations at different scales, the time series in the plot have been normalized according to $r(t) \rightarrow [r(t)-\bar{r}]/\sigma$, where $\bar{r}$ and σ denote the average and the standard deviation over the period considered, respectively.

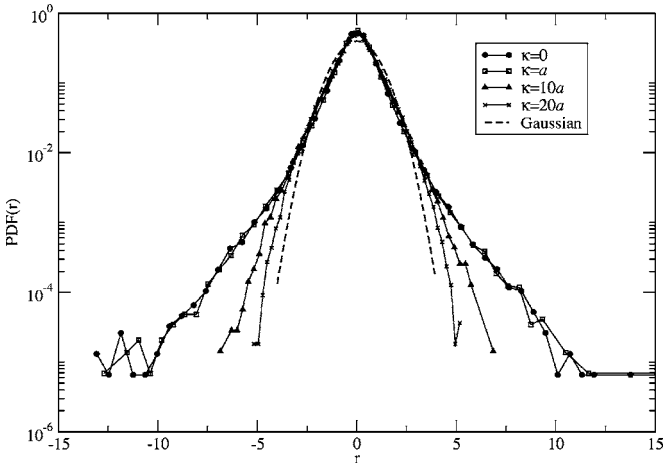

FIG. 4. The importance of the personal response related to the global opinion strength parameter κ is shown by the change of shapes of the PDFs for group interaction strength $a=1.8$. For large values of κ the time series of global opinion approaches Gaussian noise. The time series of r has been normalized—see the caption of Fig. 3.

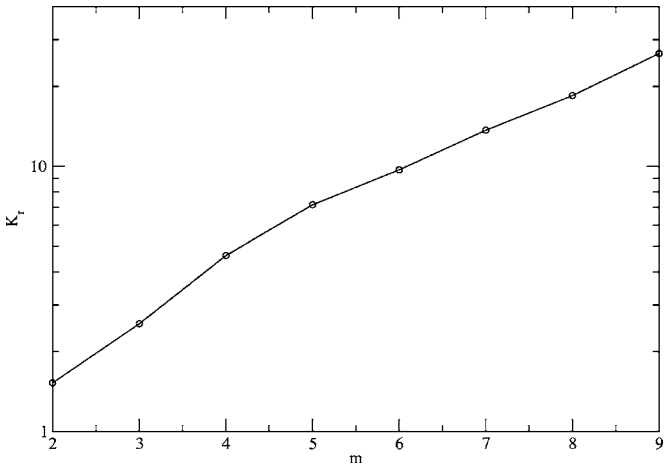

FIG. 5. Dependence of the kurtosis, defined as $K_r=\langle r^4\rangle/\langle r^2\rangle^2$, where $\langle\cdots\rangle$ denotes the temporal average, as a function of the node-edge parameter m. For a Gaussian noise process $K_r=3$ while for $K_r>3$ large deviations from the average start to appear. The final value for each m has been obtain after an average over 50 configurations of the network. The calculations show an exponential increase for K_r.

reality, the only crucial factor for the appearance of coherent events. As expected, incrementing the value of κ leads to a progressive crossover toward a noise regime. It is important to notice how this regime is reached for $\kappa>10a$. The group interactions continue to play an important role even when the average value of h_i is large compared to a.

In order to test the relevance of the network structure on the process of opinion formation, the previous simulations have been repeated, with a large number of nodes, N, and $\kappa=a$, for different values of the clustering parameter θ and the node-edge parameter m. While varying θ does not lead to any substantial difference in the dynamics of the model, the increase of the average number of links per node, $\bar{k}=2m$, has a dramatic effect in the turbulentlike phase, as shown in Fig. 5. Here the kurtosis $(K_r=\langle r^4\rangle/\langle r^2\rangle^2$, where $\langle\cdots\rangle$ denotes the temporal average) of the time series of the average opinion, used to quantify the deviation from a noise regime, is plotted against m. It is evident that an increase in the average number of links per node gives rise to more turbulence characterized by larger fluctuations and broader tails in the PDF. Large scale synchronizations are more likely to occur for large m. This behavior is intrinsically related to the model of Eqs. (2) and (3). In fact, the turbulentlike regime is a consequence of the random fluctuations of the interaction strengths between agents around a bifurcation value separating the ordered and disordered phase.

If we take the thermodynamic limit, where $N\to\infty$ and $m\to\infty$, then the coupling strengths between agents can be approximated well by the average strength over all the network and a mean field approach becomes appropriate to describe the dynamics of the model. Krawiecki *et al.* [18] proposed the following map:

$$r(t+1)=A\xi(t)r(t)+h\eta(t), \tag{5}$$

as a mean field approximation of a stochastic dynamical system similar to the one used in the present work. Here A and h are coupling coefficients and $\xi(t)$ and $\eta(t)$ random numbers in the interval $(-1,1)$. The map of Eq. (5) is a generic model for *on-off intermittency* and *attractor bubbling* extensively studied in chaos theory [24–28].

It is also worth pointing out that an increase of $\bar{k}$ is related to a decrease in the average path length between nodes; that is, the network "shrinks" and becomes more compact. In relation to our previous discussion, the more compact the network is the more the dynamics of our system approaches the mean field approximation. It becomes easier for the agents to synchronize. This characteristic of compactness, referred to as the *small world effect* [12,15,16], is actually very common in both real and artificial networks.

We further investigate the importance of the SF network topology and the small world effect in our model by performing a numerical simulation of the same system but using a *random network* (RN) or *random graph* as the underlying topology. Given a fixed a number of nodes N, a RN is defined by the probability p that two nodes are linked together [12,15,16]. In this case $\bar{k}=pN$ and, moreover, there exists a critical value $p\equiv p_c\simeq 1/N$ for which the network undergoes a topological phase transition where it moves from a phase where it is composed of a collection of small, disjoint subnetworks to a phase where a giant cluster emerges.[2] Random networks, while preserving small world properties, have a Poisson degree distribution [15] $P(k)$, and small clustering coefficients. As previously mentioned, we make use of the RN to test the robustness of our model with respect to the topology used and to learn about the most important properties relevant to the dynamics. In order to do so, we fix the

[2]Note the analogy between the random network theory and the standard percolation theory on a lattice [29] where the structural properties of the system are studied as a function of percolation probability.

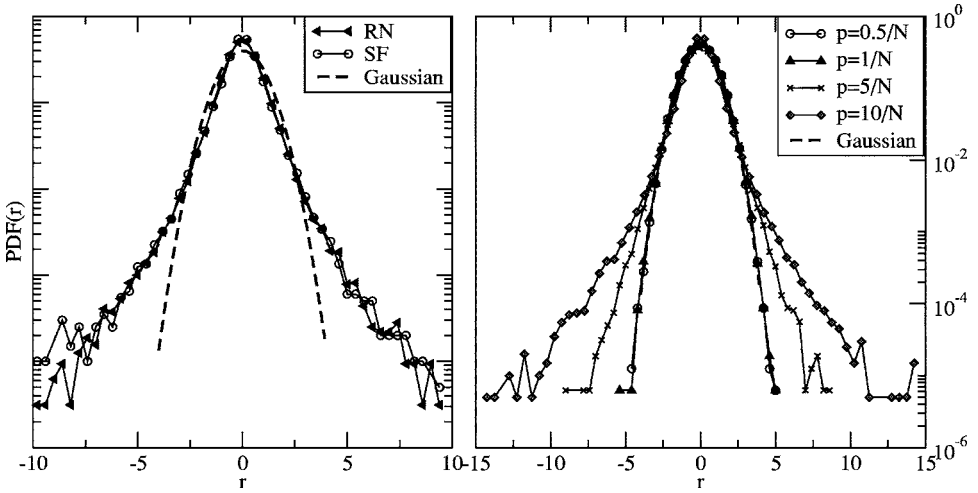

FIG. 6. Left: comparison between the PDFs of our model obtained on a SF network and on a RN with number of nodes $N=10^4$ and average links per node $\bar{k}=10$. For the SF network the parameters used are $m=m_0=5$ for the links of each new node and $\theta=0.9$ for the clustering probability while for the RN $p=10/N$. From a statistical point of view the characteristic features of the PDFs have their origin in the model dynamics as opposed to the fine features of the network. Right: Dependence of the opinion fluctuations on the parameter p on a RN. The parameters used for the dynamics are $a=1.8$ and $\kappa=a$ for the group and global opinion response, respectively.

number of agents and the average number of links for the SF and RN, namely, $N=10^4$ and $\bar{k}=10$. Then we perform independent numerical simulations on the two topologies. Note that for the RN, $\bar{k}=10$ requires $p=10/N$, which is ten times greater than the percolation threshold. The results, shown in Fig. 6 (left) demonstrate how the dynamics of the two systems are largely equivalent under the adopted constrains. In Fig. 6 (right) we also show the dependence of the dynamics on the parameter p for the RN. At the critical threshold, that is the value of p for which a giant cluster appears, there is still no trace of turbulentlike activity giving rise to fat tails. Yet in this case each agent has, on average, just one link and there cannot be any small world properties.

These results confirm that the critical topological characteristic leading to herding behavior in the framework of stochastic opinion formation is the presence of mean field effects enhanced by small world structure. The more information (links) that an agent has, the more likely it is for him/her to have an opinion in accord with other agents.

In the next section we extend our model in order to include indecision in the process of opinion formation.

IV. THE INFLUENCE OF INDECISION

We now extend our model in order to include the concept of indecision. In practice a certain agent i, at a time step t, may take neither of the two possible decisions, $\sigma_i=\pm 1$, but remain in a neutral state. Keeping faith with the spirit of the model, we address this problem by introducing an *indecision probability* ϵ: that is, the probability to find, at each time step, a certain agent undecided. This is equivalent to introducing time dependent failures in the structure of the network by setting $\sigma=0$.

Focusing on the turbulentlike regime, the shape of the PDF in the opinion fluctuations changes according to different concentrations of undecided persons. The results of the simulations, in Fig. 7, show how the dynamics of the model move from an intermittent state for $\epsilon=0$ toward a noise state for $\epsilon\approx 0.6$. The convergence to a Gaussian distribution is obtained only for quite high concentrations of undecided agents at about 60%. The robustness of the turbulentlike behavior is related to the intrinsic robustness of SF networks against random failures [14]. In fact, because there is a large absolute number of poorly connected nodes, related to the power law shape of $P(k)$, the probability of setting one of them to inactive is much higher compared to the "hubs" which are relatively rare.

We can claim that, in large social networks governed by stochastic reactions in their elements, large fluctuations in the average opinion can appear even in the case in which a

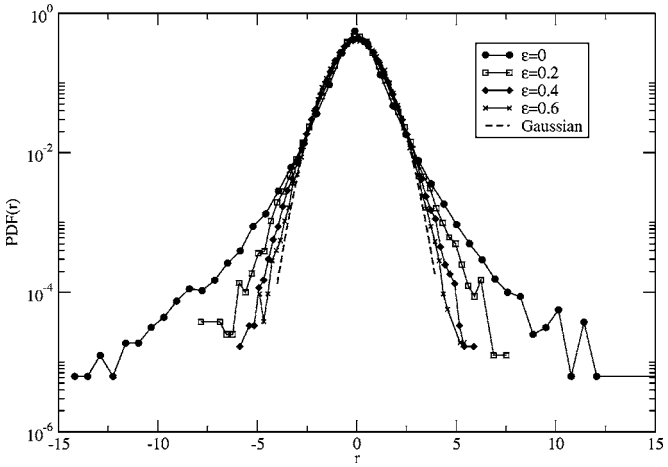

FIG. 7. Transition from coherent behavior, indecision probability $\epsilon=0$, to noise using a random selection for the inactive agents. For $\epsilon\approx 0.6$ we reach a noiselike behavior. The parameters used in the simulation are $N=10^4$ nodes, $\theta=0.9$ for the clustering probability, $m=m_0=5$ for the links of each new node, $a=1.8$ and $\kappa=a$ for the group and global opinion response, respectively.

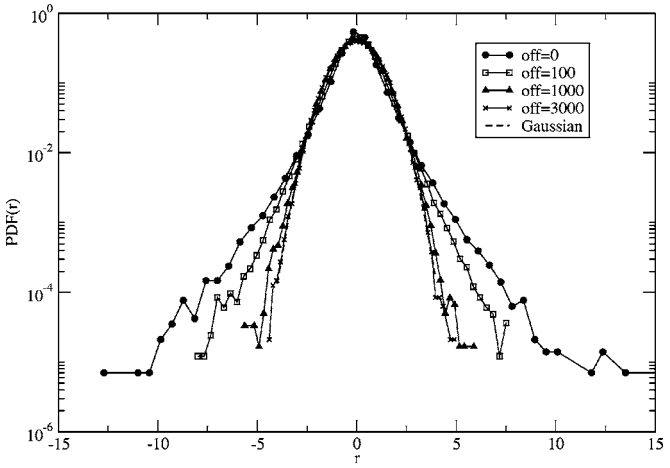

FIG. 8. In this simulation we progressively turn off the largest hubs in the network. Once we have turned off about the 10% of agents, $N=10^4$, the coherence in opinion formation disappears. The parameters used in the simulations are the same as in Fig. 7.

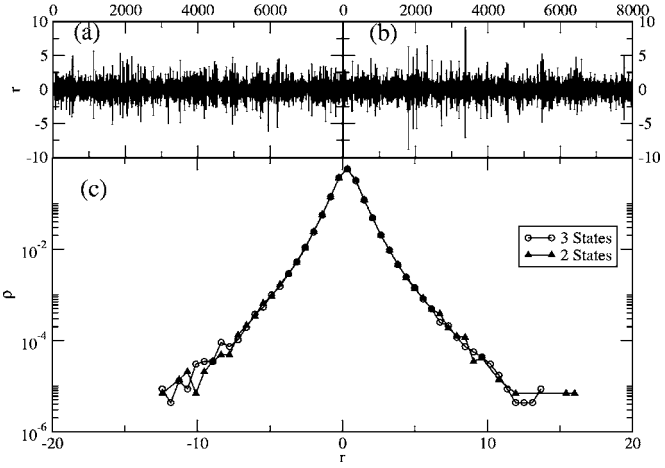

FIG. 9. (a) A window of the normalized time series generated by the two-state model with parameters $N=10^4$ nodes, $\theta=0.9$ for the clustering probability, $m=m_0=5$ for the links of each new node, $a=1.8$ and $\kappa=a$ for the group and global opinion response, respectively. (b) Window of the normalized time series generated by the three-state model with the same parameters as (a) and indecision probability width $\varsigma=1$. (c) Comparison between the PDFs generated by the two- and three-state models with the aforementioned parameters obtained over 50 realizations of the SF network. No relevant differences can be observed.

large part of the network is actually "inactive" provided that the structure is scale-free and the indecision is randomly distributed. The existence of large hubs provides for the survival of extended subnetworks in which synchronization can give rise to coherent events. The structure of the network itself supplies the random indecision.

Now we address the question of how the dynamics may change if we do not choose randomly the inactive nodes but target the nodes having the most links. What we do in practice is to sort the nodes according to their number of links and then deactivate the nodes having the largest number of links in decreasing order. Figure 8 illustrates how the fragmentation process is much faster and the noise regime is reached already when only 10% of the hubs are deactivated. As emphasized in Ref. [14], the hubs have a great importance in the structural properties of SF networks and specifically targeting these nodes can lead to sudden isolation of a large fraction of the nodes of the network.

V. AGENT INDUCED INDECISION: THE THREE-STATE MODEL

In the previous section we introduced random and targeted failures in order to study the response of the system to changes in the network topology. In a real social network the reason behind the indecision of a person follows much more complex rules and can depend on different factors as, for example, unsatisfactory information obtained by his/her sources. As seen from Eq. (3), the opinion of each agent depends on the poll of his/her network links. Suppose now that the agent i has $\tilde{N}_i$ neighbors where $\tilde{N}_i/2$ of these share the opinion $+1$ while the remaining $\tilde{N}_i/2$ share the opposite opinion. In this case, unless we give specific weights to each node, the agent i will not have an easy task in choosing one of the two possible positions because of a lack of popular consensus. Based on this idea derived from common sense, we can extend our two-state model by introducing an *induced indecision probability* μ, dependent on the information available to the agents at each time step. In particular we define the global opinion of the neighbours of the ith node as $s_i(t)=\Sigma_{j=1}^{\tilde{N}_i}\sigma_j(t)$ and the indecision probability for the ith node at time t

$$\mu_i(s,t) = c_i e^{-s_i^2(t)/2\varsigma}, \tag{6}$$

where the indecision probability width ς is a parameter of the model and c_i is a normalization constant that depends just on the structure of the network. It is calculated at the beginning of the simulation by imposing $\Sigma_{s=-\tilde{N}_i}^{\tilde{N}_i}\mu_i(s,0)=1$, i.e., the sum of the indecision probabilities over all possible global opinions to be one. The model of Eq. (6) assumes a Gaussian probability, centered in $s_i=0$, for the distribution of indecision of the ith agent. That is, the probability of having this agent in a state with $\sigma_i=0$ is greater when there is not a large agreement in the opinion of his/her sources.

The analysis of the time series generated by the three-state model does not present any relevant difference if compared with the two-state model with the same parameters, Fig. 9.

We also plot the PDF for the number of inactive agents, $N_s(t)$, during the simulation, Fig. 10. It is interesting to notice how this distribution is not Gaussian distributed around the average but is skewed on one side. Moreover, only a small fraction of agents is undecided, of the order of 10–15 %. This is consistent with the observation that in opinion polls most of the participants actually indicate an opinion.

VI. POSSIBLE APPLICATION: OPINION FORMATION AND THE STOCK MARKET

The model for opinion formation discussed thus far can be tested against the best known real social network: the

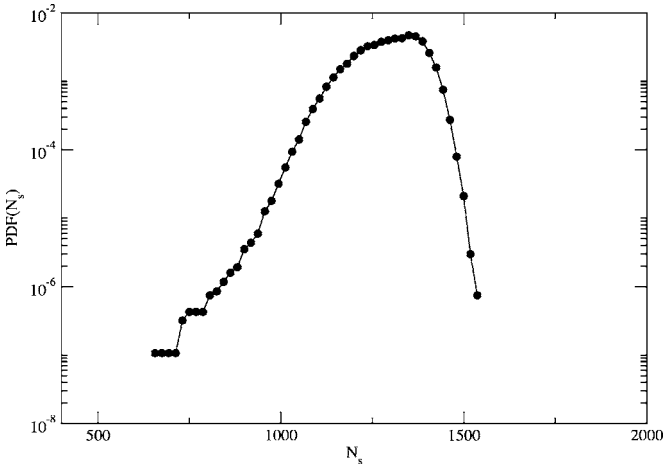

FIG. 10. PDF of the number of inactive agents, $\sigma_i(t)=0$, during the simulation of the three-state model. The parameters used are the same as used in Fig. 9.

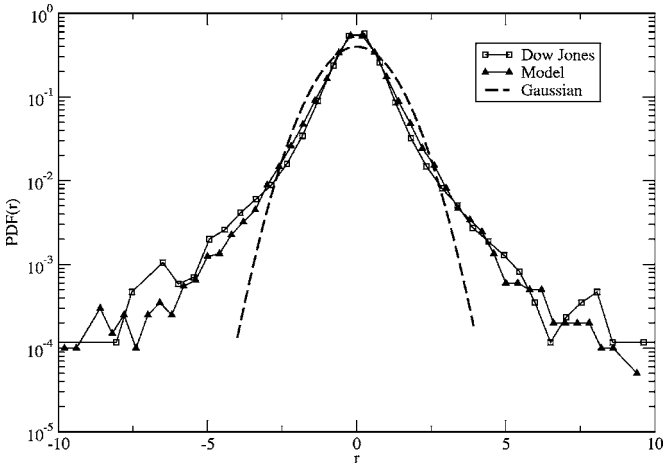

FIG. 11. Comparison between the PDF of our model and the time series of the Dow-Jones index from 13/1/1930 to 13/4/2004. The parameters of the model used to reproduce the PDF in the plot are $N=10^4$ nodes, $\theta=0.9$ for the clustering probability, $m=m_0=5$ for links of each new node, $a=1.8$ and $\kappa=a$ for the group and global opinion response, respectively. A Gaussian is also superimposed in order to emphasize the fat tails.

stock market. The main idea is to compare our results with some *stylized facts* concerning the price time series $P(t)$ and, in particular, with the properties of the logarithm of the price fluctuations, or *returns*, $R(t)=\ln P(t+1)-\ln P(t)$. In fact some characteristic features are independent of the particular market and can be considered as universal [30]. Moreover the returns show an intermittent behavior, reminiscent of hydrodynamic turbulence [30–33], also characterized by power law tails in the PDF. In this case the large coherent events are related to crashes or other anomalous variations of price.

If we assume that the variation of price is directly proportional to changes in demand and supply,

$$\frac{dP}{dt} \propto c_p P, \tag{7}$$

where c_p is proportional to the average opinion $r(t)$, then the returns are proportional to the average opinion $R(t)\approx r(t)$. Using this assumption, we compare the time series of average opinion generated by the two-state model against the time series of daily closures of the Dow Jones index. The data set spans the range 13/1/1930 to 13/4/2004 for a total of 18 645 samples. In Fig. 11, a comparison between the two PDFs is shown. The similarities between the model and the Dow Jones is remarkable. Both distributions have a *leptokurtic* shape and, in particular, they are described by power law tails, expressing the turbulentlike dynamics of the time series.[3] Note that, in contrast to the self-organized model for stock market dynamics proposed by Bak *et al.* [34], here the price feedback is not an essential ingredient for the reproduction of the correct shape of the distribution. Rather, it is the herding behavior that plays the main role, as observed from Fig. 4.

[3]The problem of the actual shape of the PDF for the stock market returns is still a matter of debate in the econophysics community [30,35]. A solution to this problem would be of great interest, especially for the practical application of option pricing.

The similarities between the artificial time series generated by the virtual social network and the stock market extend beyond the fat tails in the PDF of the fluctuations to temporal correlations. It is well known that the stock market returns have negligible correlations on daily intervals while the *volatility* ν, defined as their absolute value, have a slow power law decrease as a function of the time lag. This phenomenon is known as *volatility clustering* [30]. In order to make a comparison with our model we make use of the autocorrelation function ρ. For a time series of L samples, x_i for $i=1,\ldots,L$, this is defined as

$$\rho(\tau)=\frac{\sum_{j=1}^{L-\tau}(x_j-\bar{x})(x_{j+\tau}-\bar{x})}{\sum_{j=1}^{L-\tau}(x_j-\bar{x})^2}, \tag{8}$$

where τ is the time delay and $\bar{x}$ represents the average over the period under consideration. The autocorrelation has been computed both for the returns and for the volatility. While the time series of returns generated by the model and the Dow-Jones index have an equivalent behavior, Fig. 12 (top), the same similarities do not hold for the volatility, Fig. 12 (bottom). We observe a qualitatively different correlation: while for the market we observe a power law behavior, the memory in the time series generated by the model decays exponentially like a short-range correlated random processes [30]. This second point illustrates how nontrivial memory effects in the stock market cannot be taken into account by a simple heath bath dynamics.

In Fig. 12 (bottom) we also reproduce the autocorrelation function for the model presented in Ref. [19]. In this model a heat bath dynamics, similar to the one used in the present simulations, is applied to dynamical percolation clusters,

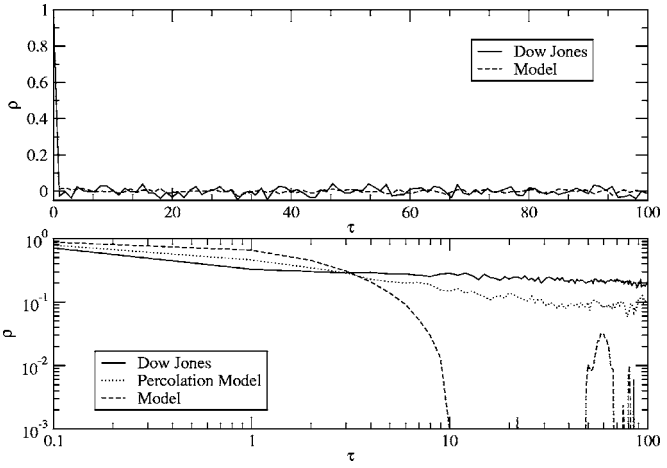

FIG. 12. Autocorrelation functions for the fluctuations r (top) and the volatility ν (bottom). The parameters used to produce the analyzed set are $N=10^4$ nodes, $\theta=0.9$ for the clustering probability, $m=m_0=5$ for the links of each new node, $a=1.8$ and $\kappa=a$ for the group and global opinion response, respectively.

used as a paradigm for agents aggregation. The temporal evolution of the clusters, whose size follows a power law distribution, is related to a forest-fire dynamics in which some potential traders are attracted in the market by other already active traders while, at the same time, some of them may temporally quit the trading. Large fluctuations in the price changes are due to the synchronization of the larger clusters in the market at a particular time. The main qualitative difference between this model and the one presented so far is that the former presents a decay rate much closer to that of the real market. At this point it is important to underline that the main difference between the two models is related to the network dynamics. While in the present simulation the network is fixed, in Ref. [19] the interactions between agents are time dependent and localized in separate clusters. We can argue that the dynamics of the networks and, in particular, the clustering of agents in different subnetworks can play an important role in the correlation properties of the stock market volatility. In reality, this fact appears quite natural if we use the autocorrelation function, defined in Eq. (8), in order to estimate the degree of memory in a process. If, for example, the variable under investigation is the sum over many independent Markovian processes, as in Ref. [19], then the resulting autocorrelation is given by the convolution of the common exponential decay, proportional to $e^{-\beta\tau}$, with the distribution of the decay rates, $g(\beta)$,

$$\rho(\tau) \propto \int_0^\infty g(\beta) e^{-\beta\tau} d\beta. \tag{9}$$

According to the shape of this distribution, the observed macroscopic variable can show a behavior characteristic of a long memory processes, like the $1/f$ Fourier spectrum [36]. Power law tails in the probability distribution function, $\rho(\tau) \propto \tau^{-\gamma}$, are produced from the distribution $g(\beta) = \Gamma(\gamma)^{-1}\beta^{\gamma-1}$, where Γ is the gamma function and γ a generic real exponent [37]. This fact strengthens the idea that the stock market is organized in a hierarchy of subnetworks where each of them can be considered, from a physical point of view, at local equilibrium. For time periods shorter than the typical time scale necessary for the networks to evolve, the only link between the subsystems composing the market is the feedback coming from the price history. This idea is closely related to the concept of *subordination* used in probability theory [38]. The superposition of distributions, as a possible explanation of fat-tailed processes, has been proposed recently by Beck [39] in the context of hydrodynamic turbulence and then extended also to other systems [40] including the stock market [41].

VII. MULTIFRACTAL ANALYSIS

Financial time series present an inherent *multifractality* [42]. In the past few years the work of many authors [19,43–46] has been addressed to the characterization of the multifractal properties of financial time series, and nowadays multifractality can be considered as a stylized fact. In order to study the multifractal properties of our model we use the *generalized Hurst exponent* [47] $H(q)$, derived via the q-order structure function,

$$S_q(\tau) = \langle |x(t+\tau) - x(t)|^q \rangle_T \propto \tau^{qH(q)}, \tag{10}$$

where $x(t)$ is a stochastic variable over a time interval T and the time delay τ. The generalized Hurst exponent, defined in Eq. (10), is an extension of the Hurst exponent H introduced in the context of reservoir control on the Nile river dam project, around 1907 [42,48]. This technique provides a sensitive method for revealing long-term correlations in random processes. If $H(q)=H$ for every q, the process is said to be monofractal and H is equivalent to the original definition of the Hurst exponent. This is the case of simple Brownian motion or fractional Brownian motion.

If the spectrum of $H(q)$ is not constant with q the process is said to be multifractal. From the definition (10) it is easy to see that the function $H(1)$ is related to the scaling properties of the volatility. By analogy with the classical Hurst analysis, a phenomenon is said to be persistent if $H(1)>1/2$ and antipersistent if $H(1)<1/2$. For uncorrelated increments, as in Brownian motion, $H(1)=1/2$. In Fig. 13 a comparison is shown between the multifractal spectra of the model and the Dow-Jones index obtained from the price time series. It is clear that both processes have a multifractal structure and the price fluctuations cannot be associated with a simple random walk as in the classical *efficient market hypothesis* [49].

VIII. DISCUSSION AND CONCLUSIONS

In the present work we have introduced a two-state model of opinion in order to simulate the complex dynamics of opinion formation in a group of individuals. The decision updating is governed by a stochastic heat bath dynamics that mimics the reaction of each person to his/her specific sources of information as governed by the network neighbors and to the average opinion of the whole group. Particular emphasis has been given to the topology of the interactions between agents, where a Barabási-Albert scale-free network has been

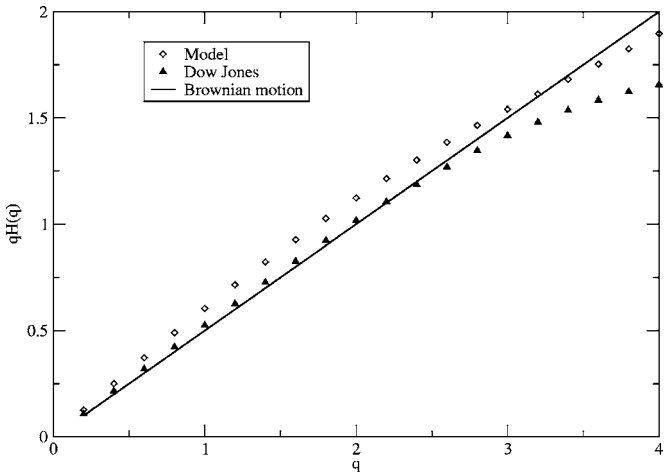

FIG. 13. Structure function exponents for the Dow-Jones index and our model. A deviation from a linear behavior is evident. The hypothetical spectrum of a one-dimensional Brownian motion is also shown for comparison.

used to simulate the links between them. The choice of this particular network is motivated by a series of recent studies on social aggregation [15,16] but, as we have shown in Sec. III, its use is not essential for the appearance of coherent events. As in other studies [17–19], we find a range in the parameter space in which the fluctuations of opinion have a nontrivial turbulentlike dynamics. The results of the simulations show that the most important factor determining the appearance of large fluctuations is the synchronization of large parts of the network. As discussed in Sec. III, this feature plays an important role even in the case in which the personal opinion is relatively strong. As a consequence large coherent events are more likely to occur when the average number of links per agent is larger.

The topology of the interactions also plays a key part in the dynamics of the model. In fact, introducing inactive agents and spreading the undecided agents randomly on the network, does not spoil the turbulentlike state even for high concentrations of "gaps," up to approximately 60% of agents. This is a consequence of the implicit robustness of SF networks against random failures. If instead of selecting randomly the undecided individuals we aim directly to the "hubs" of the network then the situation changes. In this case the network is disaggregate, composed of very small subnetworks and isolated nodes. Synchronization cannot significantly effect the resulting global opinion and the time series approximates Gaussian noise. We also introduce, in Sec. V, a three-state model. While the dynamics does not significantly differ from the two-state model, we find a persistence of opinion with a sharp upper limit in the number of undecided agents. In Sec. VI we test the results of the simulations against a time series of daily closures for the Dow-Jones index. The stock market, in fact, can be considered as the most studied network of social interactions. The results show a very good agreement with some stylized facts of the financial market like the broad tails in the PDFs, temporal correlations and a multifractal spectrum. We also notice an interesting discrepancy in the autocorrelation function for the volatility. Comparing the present results with those obtained in Ref. [19], we conjecture that the persistence in the volatility memory can be explained by considering the market as constituted by subsystems at local equilibrium and weakly interacting with each other. It will be interesting to explore this conjecture in a quantitative manner in a further investigation.

ACKNOWLEDGMENT

This work was supported by the Australian Research Council.

[1] R. J. Williams *et al.*, Proc. Natl. Acad. Sci. U.S.A. **99**, 12913 (2002); J. Camacho, R. Guimerà, and L. A. N. Amaral, Phys. Rev. Lett. **88**, 228102 (2002); J. M. Montoya and R. V. Solé, J. Theor. Biol. **214**, 405 (2002).

[2] L. A. N. Amaral *et al.*, Proc. Natl. Acad. Sci. U.S.A. **97**, 11 (2000).

[3] D. J. Watts and S. H. Strogatz, Nature (London) **393**, 440 (1998).

[4] H. Jeong *et al.*, Nature (London) **407**, 651 (2000); **411**, 41 (2001).

[5] F. Liljeros *et al.*, Nature (London) **411**, 907 (2001).

[6] M. Faloutsos, P. Faloutsos, and C. Faloutsos, Comput. Commun. Rev. **29**, 251 (1999); R. Pastor-Satorras, A. Vazquez, and A. Vespignani, Phys. Rev. Lett. **87**, 258701 (2001); S. Yook, H. Jeong, and A.-L. Barabási, Proc. Natl. Acad. Sci. U.S.A. **99**, 13382 (2002).

[7] R. Albert, H. Jeong, and A.-L. Barabási, Nature (London) **401**, 130 (1999); R. Kumar *et al.*, in *Proceedings of the Nineteenth ACM Symposium on Principles of Database Systems*, Dallas, 2000 (unpublished), p. 1. Download at http://www.sigmod.org/pods/proc00

[8] M. E. J. Newman, S. H. Strogatz, and D. J. Watts, Phys. Rev. E **64**, 026118 (2001); R. Albert and A.-L. Barabási, Phys. Rev. Lett. **85**, 5234 (2000).

[9] A.-L. Barabási and R. Albert, Science **286**, 509 (1999).

[10] S. Redner, Eur. Phys. J. B **4**, 131 (1998); A. Vasquez, Europhys. Lett. **54**, 430 (2001).

[11] G. Bonanno, G. Caldarelli, F. Lillo, and R. N. Mantegna, Phys. Rev. E **68**, 046130 (2003); J.-P. Onnela, A. Chakraborti, K. Kaski, J. Kertesz, and A. Kanto, *ibid.* **68**, 056110 (2003).

[12] B. Bollobás, *Random Graphs* (Academic, London, 1985).

[13] R. Pastor-Satorras and A. Vespignani, Phys. Rev. Lett. **86**, 3200 (2001); Phys. Rev. E **63**, 066117 (2001).

[14] R. Albert, H. Jeong, and A.-L. Barabási, Nature (London) **406**, 378 (2000); R. Cohen, K. Erez, D. ben-Avraham, and S. Havlin, Phys. Rev. Lett. **85**, 4626 (2000); D. S. Callaway, M. E. J. Newman, S. H. Strogatz, and D. J. Watts, *ibid.* **85**, 5468 (2000).

[15] R. Albert and A.-L Barabási, Rev. Mod. Phys. **74**, 47 (2002).
[16] S. N. Dorogovtsev and J. F. F. Mendes, Adv. Phys. **51**, 1079 (2002).
[17] T. Kaizoji, Physica A **287**, 493 (2000).
[18] A. Krawiecki, J. A. Holyst, and D. Helbing, Phys. Rev. Lett. **89**, 158701 (2002); A. Krawiecki and J. A. Holyst, Physica A **317**, 597 (2003).
[19] M. Bartolozzi and A. W. Thomas, Phys. Rev. E **69**, 046112 (2004).
[20] P. Holme and B. J. Kim, Phys. Rev. E **65**, 026107 (2002).
[21] Download at http://vlado.fmf.uni-lj.si/pub/networks/pajek/
[22] J. Davidsen, H. Ebel, and S. Bornholdt, Phys. Rev. Lett. **88**, 128701 (2002).
[23] Y. Kuramoto and H. Nakao, Phys. Rev. Lett. **78**, 4039 (1997); H. Nakao, Phys. Rev. E **58**, 1591 (1998).
[24] N. Platt, E. A. Spiegel, and C. Tresser, Phys. Rev. Lett. **70**, 279 (1993).
[25] E. Ott and J. C. Sommerer, Phys. Lett. A **188**, 39 (1994).
[26] P. Ashwin, J. B. Buescu, and I. Stewart, Phys. Lett. A **193**, 126 (1994).
[27] N. Platt, S. M. Hammel, and J. F. Heagy, Phys. Rev. Lett. **72**, 3498 (1994).
[28] P. Ashwin and E. Stone, Phys. Rev. E **56**, 1635 (1997).
[29] D. Stauffer and A. Aharony, *Introduction to Percolation Theory* (Taylor & Francis, London, 1992).
[30] R. N. Mantegna and H. E. Stanley, *An Introduction to Econophysics: Correlation and Complexity in Finance* (Cambridge University Press, U.K., Cambridge, 1999).
[31] R. N. Mantegna and H. E. Stanley, Nature (London) **376**, 46 (1995).
[32] S. Ghashghaie *et al.*, Nature (London) **381**, 767 (1996).
[33] R. N. Mantegna and H. E. Stanley, Physica A **239**, 225 (1997).
[34] P. Bak, M. Paczuski, and M. Shubik, Physica A **246**, 430 (1997).
[35] F. M. Ramos, Nonlinear Anal. Theory, Methods Appl. **47**, 3521 (2001); H. Gupta and J. Campanha, Physica A **309**, 381 (2002); F. Michael and M. D. Johonson, *ibid.* **320**, 525 (2003).
[36] A. Van der Ziel, Physica (Amsterdam) **16**, 359 (1950).
[37] D. Sornette, *Critical Phenomena in Natural Sciences* (Springer-Verlag, Berlin, 2004).
[38] W. Feller, *An Introduction to Probability Theory and Its Applications* (Wiley & Sons, New York, 1968), Vol. II.
[39] C. Beck, Phys. Rev. Lett. **87**, 180601 (2001); Physica A **322**, 267 (2003).
[40] C. Beck, e-print cond-mat/0502306.
[41] M. Ausloos and K. Ivanova, Phys. Rev. E **68**, 046122 (2003); N. Kozuki and N. Fuchikami, Physica A **329**, 222 (2003).
[42] J. Feder, *Fractals* (Plenum Press, New York, 1988).
[43] C. Rodrigues Neto *et al.*, Physica A **295**, 215 (2001).
[44] A. Z. Gorski, S. Drozdz, and J. Speth, Physica A **316**, 296 (2002).
[45] M. Ausloos and K. Ivanova, Comput. Phys. Commun. **147**, 582 (2002).
[46] T. Di Matteo, T. Aste, and M. M. Dacorogna, Physica A **324** 183 (2003).
[47] B. B. Mandelbrot, *Fractals and Scaling in Finance* (Springer, New York, 1997).
[48] H. Hurst, Trans. Am. Soc. Civ. Eng. **116**, 770 (1951).
[49] L. Bachelier, Ann. Sci. Ec. Normale Super. **3**, 21 (1900).